Research Square

Preprints are preliminary reports that have not undergone peer review.
They should not be considered conclusive, used to inform clinical practice,
or referenced by the media as validated information.

# Angiogenic and Immunomodulatory Effects of Hydroxyapatite Nanoparticles: A Promising Nanoplatform for Cutaneous Tissue Regeneratio

**Deena Mol Jesudhasan**
Theivanai Ammal College for Womens
**Kalaimathi Janakiraman**
jkalaimathi1978@gmail.com

Theivanai Ammal College for Womens
**Rajeshkumar Shanmugam**
Saveetha Medical College and Hospital, Saveetha Institute of Medical and Technical Sciences

**Research Article**

**Keywords:** Hydroxyapatite nanoparticles, Green synthesis, Wound healing, Scratch assay, Fibroblast cell line

**Posted Date:** July 14th, 2026

**DOI:** https://doi.org/10.21203/rs.3.rs-10078901/v1

**License:** This work is licensed under a Creative Commons Attribution 4.0 International License.
Read Full License

**Additional Declarations:** No competing interests reported.

## Abstract

# Background

Hydroxyapatite nanoparticles hold promise for use in regenerative medicine partly because of their excellent biocompatibility and calcium phosphate composition which may enhance cell migration and modulate biological responses relevant to wound healing.

# Aim

Hydroxyapatite nanoparticle synthesis and characterization was undertaken, and the potential for these nanoparticles to stimulate wound healing was examined with the use of in vitro cell line assays.

# Materials and Methods

Hydroxyapatite nanoparticles were synthesized, and their structures were characterized by microscopy and spectroscopy techniques. Cell morphology was used to qualitatively evaluate the biocompatibility of the nanoparticles. An MTT assay was used to quantitatively evaluate the biocompatibility of the nanoparticles. In this assay, cells were treated with increasing concentrations of hydroxyapatite nanoparticles, and cell viability was assessed after 24 h. The scratch assay was used to determine the in vitro wound healing potential of the hydroxyapatite nanoparticles. The scratch was visualized at time points zero and 24 h. The markers of inflammation and wound healing, VEGF and FGF, and cytokines IL-4 and IL-1β, respectively, were measured using the qRT-PCR technique.

# Results

TEM images show hydroxyapatite nanoparticles exhibiting a size range of 10–25 nm and an aggregated structure. SEM and AFM images show rough and granular surface topography of the nanoparticles and EDX showed signals for calcium, phosphorus, and oxygen. The nanoparticles were cytocompatible as the cell viability was greater than 90% for all concentrations tested. Nanoparticle treatment in scratch assays resulted in improved cell migration and decreased wound gaps. There was an increase in the gene expression of VEGF, FGF, and IL-4 and a decrease of IL-1β.

# Conclusion

The hydroxyapatite nanoparticles that were synthesized are biocompatible and support the process of migration during wound healing and the modulation of gene expression in the process of wound healing. The nanoparticles may be appropriate for use as nanobiomaterials in the fields of tissue engineering and regenerative medicine.

# Introduction

Wound healing relies on a multi-step process that includes hemostasis, inflammation, proliferation, and the formation of new blood vessels, deposition of the extracellular matrix, and remodeling of the tissue(1). There are also many key functions, crossing many phases, such as fibroblast migration, proliferation, collagen synthesis, and the regulation of inflammation that are key to effective closure of a wound(2). If the aforementioned processes are disrupted, the wound healing may be delayed, and result in chronic wounds, invasion from microbes, and worsening inflammation and poor tissue restoration. Therefore, in the field of regenerative medicine, the need is to create and develop safe and biocompatible engineered materials that sustain cell migration and that can control the inflammatory response to heal the wound(3).

Current methods for managing wounds include topical antibiotics and antiseptics, wound dressings, growth factors and polymer-based wound therapies. Most of these methods have poor interactions and delays with tissue, cellular response, stability, and regeneration; as well as resistance to antimicrobials(4, 5). Recently, nanotechnology-based biotherapies have been incorporated into the management of wounds. These therapies improve interaction and response with biological systems and can be tailored to wound healing(6, 7). Nanoparticles can be used to influence cellular behavior and strengthen interactions of cells and extracellular matrices, further enhance growth factors, and control inflammation(8, 9).

Calcium phosphate ocurring naturally as a mineral with a chemical formula of $Ca_{10}(PO_4)_6(OH)_2$ occurs commonly as a major inorganic component of bones and teeth. Hydroxyapatilte has great biocompatibility and can be used in combination with other polymers to enhance their osteoconductivity(10). Hydroxyapatite can be emdedded in scaffolds and other polymers to control the rate of drug release. Hydroxyapatite has applications beyond hard tissues, in soft repair and regeneration of tissues and in the signaling of tissue repair and regeneration.(11).

Compared to bulk hydroxyapatite, hydroxyapatite “nanoparticles have several advantages. Their nanoscale size results in higher surface-to-volume ratio, increasing interactions with cells and biological molecules(12). Hydroxyapatite nanoparticles have a surface chemistry that favors protein adhesion along with the adsorption of growth factors potentially aiding cell adhesion and migration. In addition, hydroxyapatite has the ability to release calcium and phosphate ions and may aid in cell signaling and the regulation of the extracellular matrix. These properties support the use of hydroxyapatite nanoparticles in developing advanced wound healing systems that require cell compatibility and tissue regeneration(13, 14).

The green synthesis approach has appeared in recent years to prepare metal and mineral nanoparticles in a biocompatible, inexpensive, and environmentally friendly manner. In this work, hydroxyapatite nanoparticles were prepared using the green synthesis method assisted by the plant extracts of Calendula officinalis and Camellia sinensis(15–17). Compared to all of the other methods, plant-mediated synthesis has the advantage that many of the phytochemicals present in plant extracts can

play multiple roles during the preparation of nanoparticles, performing the functions of reducing, stabilizing, and capping agents(18, 19). The plant extracts contain many different biomolecules including polyphenols, flavonoids, tannins, terpenoids, alkaloids, proteins, and organic acids, all of which can assist in nucleation and stabilization of the hydroxyapatite nanoparticles and can help control the growth of the hydroxyapatite. The use of plant extracts can also eliminate the use of harsh chemicals and improve the biocompatibility of the hydroxyapatite nanoparticles, which assists in their application for tissue engineering and for use in wound healing(20, 21).

Calendula officinalis is a well-known traditional medicine for treating wounds due to its anti-inflammatory, antioxidant, and antimicrobial properties(22). Bioactive constituents such as flavonoids, triterpenoids, phenol compounds, and carotenoids are reported to aid tissue repair, and stimulate collagen formation and regulation of inflammation. Camellia sinensis, known as green tea, is another example of a plant that contains catechins, polyphenols, and flavonoids, as well as other molecules that are antioxidants and are reported to protect cells from oxidative stress and support the regeneration of stressed cells(23). The integration of Calendula officinalis and Camellia sinensis extract for the synthesis of hydroxyapatite nanoparticles may offer the initial support for the formation of hydroxyapatite nanoparticles and the final nanomaterial with phytochemicals. The surface interactions and phytochemical coatings may enhance the cytocompatibility, cell migration, anti-inflammatory, and wound healing activities of the hydroxyapatite nanoparticles that were synthesized(24, 25).

Given the dual importance of hydroxyapatite in biology and as a component of an effective wound healing biomaterial, we synthesized and assessed hydroxyapatite nanoparticles and their in vitro wound healing potential using cell line models. The synthesized nanoparticles were analyzed to determine their morphology, size, elemental constituents, and surface topography. Cell morphology analysis and the MTT assay were employed to evaluate the cytocompatibility of the nanoparticles. The scratch assay was conducted to evaluate the wound healing potential, and the expression of the wound healing associated genes, VEGF, FGF, IL-4, and IL-1β, was evaluated. Based on the results, hydroxyapatite nanoparticles hold the potential to be a nanobiomaterial for wound healing and tissue regeneration.

## Materials and methods

# Materials

The chemicals used for the study were calcium nitrate tetrahydrate, diammonium hydrogen phosphate, sodium hydroxide, phosphate buffered saline (PBS), Dulbecco's modified Eagle Medium (DMEM), fetal bovine serum (FBS), antibiotic-antimycotic, trypsin-EDTA, MTT and DMSO. All chemicals were of analytical and reagent grade and used as such. The fibroblast cell line was used in the in vitro biocompatibility and wound healing assays.

## Synthesis of hydroxyapatite nanoparticles

Nanoparticles of hydroxyapatite were synthesized by a hydro-solvothermal route. Firstly, a calcium “precursor solution was prepared by dissolving calcium nitrate tetrahydrate in distilled water. Separately, a phosphate precursor solution was prepared by dissolving diammonium hydrogen phosphate in distilled water. Phosphate solution was added drop-wise to the calcium solution while magnetically stirring the solution. To control the pH, and in order to promote the formation of a hydroxyapatite precipitate, sodium hydroxide solution was used to make the reaction mixture alkaline. A white precipitate formed after magnetically stirring the mixture at room temperature for some time. The white precipitate was collected by centrifugation, and washing to remove impurities. The precipitate was dried and powdered for further characterization and biological studies.

## Characterization of hydroxyapatite nanoparticles

The synthesized hydroxyapatite nanoparticles were characterized using a number of analytical techniques. The size and morphology of the nanoparticles was done using transmission electron microscope. The morphology of the surface was studied using a scanning electron microscope. The surface element composition was studied using energy dispersive X-ray spectroscopy. The surface of the synthesized nanoparticles was studied for topography and roughness using atomic force microscopy. The nanoparticle powder was mounted on sample holders and analyzed under standard instrumental conditions.

## Cell culture maintenance

Fibroblast cell lines were maintained in DMEM with 10% Fetal bovine serum and 1% antibiotic-antimycotic and incubated at 37°C in a humidified incubator containing 5% $CO_2$. For sub culturing, cells were detached using trypsin-EDTA once 70–80% confluency was achieved. For biocompatibility, cytotoxicity, scratch assay, and gene expression analysis, actively growing and healthy cells were used.

## Morphological assessment of biocompatibility

Cellular morphology was employed as an initial method to assess the biocompatibility of hydroxyapatite nanoparticles. Fibroblast cells were seeded, and allowed to adhere for one hour, and were then exposed to hydroxyapatite nanoparticles at 36 µg/mL and 72 µg/mL. Control groups were established using untreated cells. Phase contrast microscopy was then employed to observe and capture nanoparticle induced changes to cell morphology such as cell density, attachment, rounding, shrinkage, and cell detachment.

# MTT assay for cytocompatibility

To assess the cytocompatibility of hydroxyapatite nanoparticles, the MTT assay was performed. Fibroblast cells were seeded in 96 well microplates and treated with hydroxyapatite nanoparticles at

varying concentrations (0.1–300 µg/mL) after an overnight cell adhesion incubation. Cells were then incubated with the hydroxyapatite nanoparticle treatment for 24 hours. Formazan crystals were allowed to form after the addition of MTT solution and an incubation period. The medium" was then removed and the formazan crystals were dissolved with DMSO. Absorbance was then measured using a microplate reader. Cell viability was calculated using the following equation:

## Cell viability (%) = (Absorbance of treated cells / Absorbance of control cells) × 100

The $IC_{50}$ value was calculated using linear regression analysis.

## In vitro scratch wound healing assay

Hydroxyapatite nanoparticles were tested for their wound healing potential using an in vitro scratch assay. Fibroblast cells were grown until reaching a confluent monolayer. A scratch was made on the cell monolayer using a sterile pipette tip. Monolayer was rinsed with sterile PBS to remove detached cells. Hydroxyapatite nanoparticles were added at concentrations of 36 µg/mL and 72 µg/mL. Untreated scratched cells were used as the control. Wound areas were photographed using an inverted microscope at scratch formation time (0 h) and after a 24 h incubation period. First, 0 h and 24 h photographs were used to assess cell migration and wound closure.

# Gene expression analysis by qRT-PCR

To assess the impact of hydroxyapatite nanoparticles on the expression of genes associated with wound healing, we utilized quantitative real-time PCR (qRT-PCR). Cells were exposed to hydroxyapatite nanoparticles at concentrations of 36 µg/mL and 72 µg/mL, and nanoparticles were not applied to some cells and these cells were used as control. Following treatment, RNA from the cells was isolated using a reagent for the RNA isolation. The integrity, quality and concentration of isolated RNA were analyzed using a spectrophotometer. Messenger RNA was reverse transcribed to cDNA. The expression of VEGF, FGF, IL-4, and IL-1β was analyzed using qRT-PCR. The expression of genes was evaluated using a housekeeping gene as an internal control. The relative changes in gene expression was analyzed using the comparative Ct method. The expression of genes was analyzed by fold change with respect to the control, which was the untreated group.

# Statistical analysis

All experiments were conducted in triplicate and the data presented as mean ± SD. Calculations were performed using statistical analysis software. Control and treated groups were compared using one-way analysis of variance. Statistically significant differences were determined at a p value < 0.05. The results were considered significant" when *p < 0.05, **p < 0.01, and ***p < 0.001.

## Results

# TEM Analysis of Hydroxyapatite Nanoparticles

In order to examine the morphology, particle size, and structure of the synthesized hydroxyapatite nanoparticles within the nanoscale, transmission electron microscopy was utilized. The formation of nanoparticles which appeared to be aggregated and had irregular flake-like morphology is shown in Fig. 2. The particles appeared to be compact clusters of several small crystalline domains. The nanoparticles showed a faint needle-like and plate-like morphology at higher magnification which are typical of hydroxyapatite nanostructures.

The primary hydroxyapatite nanoparticles were around 10–25 nm in size, based on the 20 nm scale bar. However, due to extreme agglomeration, individual particle boundaries were unclear in most areas. This aggregation is likely due to the high surface energy of hydroxyapatite particles and potential calcium and phosphate interactions during hydroxyapatite nanoparticle synthesis. The areas in the dark contrast in the images are areas of high particle density and areas of overlapping hydroxyapatite nanoparticle clusters. The light contrast areas are the regions of dispersed hydroxyapatite nanoparticles.

The particle size and the morphology of the hydroxyapatite nanoparticles, as confirmed by TEM analysis, was in the range of 10–25 nm. The nanoparticles possess a agglomerated structure, which is surmised to be beneficial in the field of biomedicine. This is due to the fact that hydroxyapatite nanoparticles, in the given size range and structure, have the potential to increase surface area and, therefore, enhance the attachment of cells and the interactions with components of the extracellular matrix and promote cellular migration in the process of wound healing.

# SEM analysis

The morphology of hydroxyapatite nanoparticles was studied with the aid of scanning electron microscopy (SEM). The particles were irregularly shaped and highly aggregated with a rough surface (Fig. 3A). At low magnification, the surface morphology was dominated by clusters of strongly agglomerated particles with rough, uneven distribution. This is likely due to strong interactions between particles and the high surface energy of nano-hydroxyapatite.

At higher magnifications, it was observed that the surface of the hydroxyapatite particles displayed rough, tubular, and partially flake-like surfaces (Fig. 3B). This surface was highly interconnected and packed with microstructures indicating a high degree of particle aggregation at the nanostructural level. This type of surface morphology of hydroxyapatite is likely to be beneficial for cellular interactions, as it may serve as a good surface for the attachment of cells, the deposition of extracellular matrices, and the migration of fibroblasts, which are important for the process of wound healing.

From the scanning electron micrographs, the hydroxyapatite nanoparticles were confirmed to be highly aggregated with rough and porous microstructure. This type of morphology of hydroxyapatite

nanoparticles is likely to be beneficial for cellular adhesion and for stimulating the healing of wounds in vitro.

# SEM & EDX

Elemental analysis of synthesized hydroxyapatite nanoparticles was done using scanning electron microscopy (SEM) integrated with energy dispersive X-ray spectroscopy (EDX). Based on morphological assessment of the selected SEM image for elemental analysis (Fig. 4A), a distinct hydroxyapatite particle possessing irregular crystalline morphology was observed. The sample included compact angular structures surrounding smaller aggregates, which suggested the presence of mineralized hydroxyapatite domains.

The EDX spectrum in Fig. 4B illustrates signals for the principal constituents of hydroxyapatite, which are calcium, phosphorus, and oxygen. From the spectra, it was confirmed that calcium phosphate-based hydroxyapatite nanoparticles were formed. Peaks for Ca and P were of special interest as these elements are the major inorganic constituents of hydroxyapatite. The oxygen peak was indicative of the contribution of hydroxyl and phosphate to the hydroxyapatite structure.

As major constituents, Ca and P and O were accompanied with small signals of C and some minor trace elements. The peak for carbon could be due to carbon tape, the sample holder, or some organic residues that were left during the sample prep. Detection of minor trace elements could be due to impurities of the precursors used or background noise of the instrumentation. EDX analysis in total substantiated that the synthesized nanoparticles were predominantly of calcium, phosphorus, and oxygen, which confirmed the synthesis of hydroxyapatite nanoparticles.

Atomic force microscopy (AFM) was utilized to analyze surface topography and surface roughness of the synthesized hydroxyapatite nanoparticles. AFM imaging in two dimensions showed a rough surface at the nanoscale with elevations and depressions (Fig. 5A). Analyzed in height, the surface showed irregular, rough, and depressions at the nanoscale with variable spacing. The roughness analysis showed irregularity in the surface architecture, which could be attributed to the aggregation of hydroxyapatite nanoparticles and formation of dense, compact nanoscale regions.

From the three-dimensional AFM imaging (Fig. 5B), the irregularity in surface morphology of synthesized hydroxyapatite nanoparticles was visible. Sharp peaks and valley regions indicate an irregular arrangement of the nanoparticles in the scanned region. The sharp and compact surface morphology indicates that the hydroxyapatite nanoparticles formed an aggregated surface with an increased roughness. This surface morphology, which is irregular and rough, is beneficial for biomedical applications because it increases the surface area for cellular interactions and adsorption of proteins and the extracellular matrix.

In summary, all AFM analysis of the nanoparticles showed a rough surface morphology that was irregular in granularity. This morphology was corroborated in the SEM and TEM analyses and is expected to enhance cellular adhesion and promote cellular migration for improved wound healing.

# Biocompatibility analysis

The synthesized hydroxyapatite nanoparticles were evaluated for biocompatibility by assessing cellular morphology in the treated cell line. As seen in (Fig. 6A), untreated control cells displayed normal adhesive growth along with the typical spindle and elongated fibroblast-like cell morphology, indicating the presence of a healthy cellular architecture. The cells had well-defined boundaries and displayed no cellular damage.

Cell treatment with hydroxyapatite nanoparticles at a concentration of 36 µg/mL (Fig. 6B) showed no morphological changes compared to the control. The treated cells remained adhesive to the substrate, and the extensions of the cells suggested that the nanoparticles at this concentration did not induce any major cytotoxic effects. Shrinkage of the cells, disruption of the cell membrane, and severe detachment of cells were not observed.

Cells treated with hydroxyapatite nanoparticles at 72 µg/mL retained adhesion and fibroblast-like cell morphology, although, compared to the control group, cell density was reduced (Fig. 6C). Most of the treated cells appeared to be viable, with cell extensions and only minor changes in cell morphology, supporting the conclusion that hydroxyapatite nanoparticles had excellent cytocompatibility for the concentrations evaluated.

Hydroxyapatite nanoparticles did not cause any major cellular damage to the treated cell line, as evaluated by morphology. For both 36 and 72 µg/mL treatments, cell attachment and cell morphology were preserved, indicating biocompatibility of the synthesized nanoparticles and supporting the use of these nanoparticles for evaluation of potential therapeutic activity in wound healing.

# Cytocompatibility assessment by MTT assay

To see how the synthesized hydroxyapatite nanoparticles interact with cells, compatibility testing was conducted using the MTT assay after 24h treatment. Decreasing cell viability was evident as the concentration of the nanoparticles increased (Fig. 7A). The concentration demonstrating 50% inhibition was found to be 36.79 µg/mL using linear regression to estimate the $IC_{50}$ value. Synthesized hydroxyapatite nanoparticles showed low cytotoxicity as cell viability was maintained at > 90% even at the highest concentrations tested.

Cell viability after treatment with varying concentrations of nanoparticles is illustrated in Fig. 7B. Maximal cell viability was observed in control cells and in cells treated with lower concentrations of hydroxyapatite nanoparticles. Concentrations of hydroxyapatite nanoparticles between 0.1 and 30 µg/mL showed no significant toxic effect and a high level of cell viability was maintained. Cell viability was decreased to a small extent at hydroxyapatite concentrations of 100 and 300 µg/mL. Cell viability at these concentrations was still > 90% indicating good cytocompatibility.

Data from the MTT assay at all of the tested concentrations indicated that hydroxyapatite nanoparticles were biocompatible. The data indicated that these nanoparticles should be suitable for use in evaluating

the wound healing potential of an in vitro cell line model.

## In vitro wound healing activity by scratch assay

In vitro scratch assays were performed to assess the potential of the synthesized hydroxyapatite nanoparticles to heal wounds. Figure 8 shows representative images of the scratch area at the 0 h and 24 h time points. For the 0 h time point, the untreated control group (Fig. 8A) showed a clearly defined scratch with no cells present in the scratch area. The 0 h time point images for the treatments with hydroxyapatite nanoparticles at concentrations of 36 µg/mL (Fig. 8B) and 72 µg/mL (Fig. 8C) also showed clearly defined scratch areas with visible gaps in the scratch.

The untreated control group (Fig. 8D) showed some closure of the scratch due to cell migration, but a large scratch gap remained, demonstrating low closure. The group treated with hydroxyapatite nanoparticles at a concentration of 36 µg/mL (Fig. 8E) showed a large reduction in scratch width due to substantial cell migration and/or improved closure. The group treated with hydroxyapatite nanoparticles at a concentration of 72 µg/mL (Fig. 8F) also showed large improvements in closure and migration compared to the control.

Among the tested groups, hydroxyapatite nanoparticles assisted in the formation of 24-hour visible wound closure, possibly due to their capacity to stimulate cell migration. The nanoparticles' promoted cell migration could be due to hydroxyapatite's composition of calcium phosphate, nanoparticles, and their biocompatible nature that potentially aid cell attachment and possibly enhance the process of tissue regeneration. The scratch-assay results confirmed that hydroxyapatite nanoparticles stimulated cell migration, and thus, they are promising agents for wound healing.

## Gene expression analysis of wound healing markers

The effect of hydroxyapatite nanoparticles on the expression of VEGF, FGF, IL-4, and IL-1β was assessed by measuring the relative fold changes. Hydroxyapatite nanoparticle-treated cells expressed significantly higher levels of VEGF compared to the control group (Fig. 9A). VEGF expression increased to about 1.7-fold in the 36 µg/mL treatment, and to nearly 2.7-fold in the 72 µg/mL treatment. This suggests that hydroxyapatite nanoparticles may facilitate the signaling of angiogenesis during the process of wound healing.

As shown in Fig. 9B, nanoparticle treatment also resulted in increased expression of FGF. Cells treated with 36 µg/mL and 72 µg/mL expressed FGF to about 1.7-fold and 2.8-fold, respectively. Since FGF is critical for the initiation and formation of the extracellular matrix and tissue healing, this result further suggests the hydroxyapatite nanoparticles' capacity to enhance the healing of wounds.

Also, the expression of IL-4 was significantly higher in treated cells compared to the control (Fig. 6C). Compared to the control, the 36 µg/mL and 72 µg/mL treatment groups expressed IL-4 to about 1.6-fold and 2.6-fold, respectively. This indicates that hydroxyapatite nanomaterials may have the capacity to modulate the immune response, which is associated with the healing and regulation of inflammation.

Hydroxyapatite nanoparticles inhibited IL-1β expression, shown in Fig. 6D. At 36 µg/mL, expression fell to about 0.7, and to about 0.3 at 72 µg/mL. This may indicate that hydroxyapatite nanoparticles inhibit the promotion of signaling of inflammation in consideration of the other data available and may create a microenvironment that favors the promotion of healing.

Overall, Gene expression analysis indicated that hydroxyapatite nanoparticles increased the expression of pro-angiogenic and healing factors, IL-4, VEGF, and FGF, and decreased the expression of the pro-inflammatory factor IL-1β. This may indicate that the hydroxyapatite nanoparticles may be beneficial for healing of wounds and tissue healing due to their pro-angiogenic and pro-fibroblast activities, and their anti-inflammatory effects.

# Discussion:

From the findings of this investigation, hydroxyapatite nanoparticles (nHAp) emerge as a highly attractive nanobiomaterial for the healing of wounds and tissue regeneration. This is likely the result of a combination of beneficial physicochemical properties and an ability to elicit a directed biological response(26). The range of “dimensions (10–25 nm) observed using Transmission Electron Microscopy (TEM) confirm that nHAp has a greater surface area than the bulk material. This increase in surface area leads to an increase in the potential for bioactivity. The surface of the nHAp is rough and porous and exhibits a flaky morphology (Fig. 1); this is not merely a detail of the morphology, it is an advantageous function that provides a matrix which is a more biomimetic representation of the natural extracellular matrix (ECM)(27). The improvement of the biomimetic interface of the material will also improve the initial interactions of the cells with the material and promote the adhesion and spreading of the cells, and the overall migration that is vital in the healing process(28).

The ability of the synthesized nHAp to maintain cell viability above 90% in the MTT assay and to preserve the normal morphology of fibroblasts demonstrates its cytocompatibility and reinforces its potential use for therapeutic applications. This property of low cytotoxicity can be attributed to the biocompatibility of hydroxyapatite. Given that the chemical composition of hydroxyapatite ($Ca_{10}(PO_4)_6(OH)_2$) is nearly the same as that of the mineral component of human bones and teeth(29, 30). This compositional similarity aids the human body in the perception of nHAp as a "self" material, leading to low immune response and favorable conditions for cellular activities. The successful formation of the calcium phosphate structure concluded by EDX is evidence for this biocompatibility being a result of the material's intrinsic chemistry(31, 32).

The application of nHAp for the enhancement of the healing of wounds was further validated by the in vitro scratch assay. The addition of nHAp to the wound site was observed to speed up the closure of the wound by inducing greater migration of fibroblasts. This is of great importance as fibroblasts are responsible for the synthesis of the extracellular matrix (ECM) to facilitate the healing of the wound, and their migration into the wound site is critical for the formation of granulation tissue and the process of epithelial healing(33, 34).

First and foremost, the gene expression investigation helps elucidate the mechanisms underlying the observed phenotypic effects, demonstrating that nHAp coordinates a complex molecular program supportive of tissue repair. Of great interest is the expression of VEGF and FGF(31). VEGF is the key regulator of the process of making new blood vessels, which is crucially important for bringing new blood to a healing wound (along with immune cells) and supplying it with the nutrients and oxygen essential to the process. FGF, on the other hand, promotes the proliferation and recruitment of fibroblasts and endothelial cells, offering direct support for the results of the scratch assay(35, 36). The application of a shifting (modifying) inflammatory response, with IL-4 and IL-1β levels, represents a highly sophisticated and desirable effect. IL-4 is a classical anti-inflammatory cytokine that is involved in the transition of the inflammatory phase of healing to the proliferative phase, which is involved in the remodeling and the healing of the tissue, whereas in direct opposition to IL-1β, the presence of which is characteristic of non-healing chronic wounds, and which is a major inflammation-inducing cytokine(37, 38). nHAp seems to be providing signals to facilitate/regenerate the microenvironment of the wound in the direction of productive healing by increasing the regenerative signals of (VEGF and FGF) and decreasing the damaging signals of inflammation (by the reduction of IL-1β and increase of IL-4).

Individually each of the results leads to an important understanding centering on the nanoscale size and roughened surface of nHAp as a scaffold for cell interaction, safe host response through its biocompatibility, the promotion of fibroblast migration as an important cellular event for tissue repair, and the regulation of critical growth factors and cytokines as a strong molecular stimulus for angiogenesis, tissue repair, and the resolution of inflammation (39). These in vitro results are strong and very encouraging, but are only the beginning. The next steps in this series should include important quantitative assessments of wound closure and, most importantly, well conceived in vivo studies in appropriate animal models. These studies are needed to ensure that nHAp will promote the desired outcome of tissue repair and regeneration as a therapeutic agent in the evolving and complex environment of a living organism. In this environment the effects of cell stimulation, tissue response and repair, and the regulation of inflammation through the control of blood vessel growth and the clearance of cellular debris will be evident.

# Conclusion

This study showed that hydroxyapatite nanoparticles may have good potential for wound healing in an in vitro cell line model. Characterization by TEM, SEM, and AFM showed that the synthesized nanoparticles were in the nanoscale with a rough, porous, and irregular, aggregated, granular surface and had a size of 10–25 nm. EDX detected calcium, phosphorus, and oxygen, confirming the fabrication of calcium phosphate-based hydroxyapatite nanoparticles. The biocompatibility of the nanoparticles was confirmed by the normal adherent morphology of the treated cells and a cell viability of over 90% for all tested concentrations. The scratch assay showed improved” cell migration and a reduced wound gap for the nanoparticle treated groups, when compared to the untreated control cells, indicating improved activity for the closure of the wound. Moreover, the upregulation of VEGF, FGF, and IL-4, the downregulation of IL-1β, and the overall results, indicate that hydroxyapatite nanoparticles may promote wound healing by

stimulating angiogenic and regenerative signaling, and by suppressing inflammation. The overall results support that hydroxyapatite nanoparticles are biocompatible and can support the cellular migration and the repair of wounds. Thus, they may be nanobiomaterials for wound healing and tissue repair in regenerative medicine. Further studies in vivo are needed to assess their therapeutic potential.

## Declarations

# Author Contribution

DM: Writing – original draft, Validation, Methodology, Investigation, Formal analysis, Data curation. Validation, Methodology, and editing with review of the manuscript, Data curation, and Visualization. KJ & RS: Writing – review & editing, Validation, Supervision, Methodology, Investigation, Data curation, Conceptualization.

## References


1. Essa, S. H., Mohammad, S. Q., Kadhum, D. A., & Jalil, I. S. (2024). Effectiveness of silver nanoparticles as antibacterial agents with natural wound healing cream with extracted Aloe vera gel. *Regul Mech Biosyst*, *15*(4), 821–825.
2. Wu, T., Xu, Z., Yi, G., Wang, D., Chen, S., Zhang, S. (2026 June;36(44)). Microenvironment-responsive nanozyme for all stages of infectious chronic wound management through macrophage reprogramming. Adv Funct Mater [Internet]. Available from: http://dx.doi.org/10.1002/adfm.75099
3. Jreije, S., Fadel, M., Karam, C., Ghadieh, H. E., & Ghanem, A. (2026 June). Diabetes and delayed wound healing: Molecular mechanisms and dermatological interventions. *International Wound Journal*, *23*(6), e70972.
4. Karadeniz, O., Guler, O. M., Tunc, B., & Goksu, M. (2026). Negative pressure wound therapy versus conventional debridement in subcutaneous abdominal wound healing in obese patients following obstetric/gynaecologic surgery. *Journal Of Wound Care*, *35*(Sup4a), S18–26.
5. Essa, M. S., Ahmad, K. S., Zayed, M. E., & Ibrahim, S. G. (2023). Comparative study between silver nanoparticles dressing (SilvrSTAT Gel) and conventional dressing in diabetic foot ulcer healing: A prospective randomized study. *The International Journal Of Lower Extremity Wounds*, *22*(1), 48–55.
6. Wu, J., Zhang, B., Lin, N., & Gao, J. (2023). Recent nanotechnology-based strategies for interfering with the life cycle of bacterial biofilms. *Biomater Sci*, *11*(5), 1648–1664.
7. Kumar, S., Nehra, M., Kedia, D., Dilbaghi, N., Tankeshwar, K., & Kim, K-H. (2020). Nanotechnology-based biomaterials for orthopaedic applications: Recent advances and future prospects. *Materials Science & Engineering. C, Materials For Biological Applications*, *106*(110154), 110154.
8. Haque, S. T., Saha, S. K., Haque, M. E., & Biswas, N. (2021). Nanotechnology-based therapeutic applications: in vitro and in vivo clinical studies for diabetic wound healing. *Biomater Sci*, *9*(23), 7705–7747.

9. Kalaimathi, J., Sridevi, B., Ananthi, S., Nasrin, J., Suriya, M., & Rajeshkumar, S. (2019). Glycine max seed mediated synthesis and characterization of zinc oxide nanoparticles and its antifungal activity against pathogenic fungal strains. *Indian J Public Health Res Dev*, *10*(11), 3628.
10. Gupta, S., Shetty, T., & Rodrigues, S. (2026 Sept). Emerging technologies in hydroxyapatite coating over Zirconia implants: A comprehensive review. *Biomed Mater Devices*, *4*(3), 2721–2731.
11. Yadav, M. M., Dasankoppa, F. S., Adinarayanappa, S. M., Sholapur, H. N., Umarfarooq, M. A., Sagare, R. D., et al. (2026 Sept). Surface functionalization of silicon carbide with chitosan and hydroxyapatite for bioactive wound healing and tissue regeneration. *Journal Of Drug Delivery Science And Technology*, *123*(108455), 108455.
12. Yang, W., Xu, H., Chen, Z., Du, Y., Qian, X., Wu, X., et al. (2026 July). Synthesis of mesoporous cerium-doped hydroxyapatite nanoparticles for efficient and selective defluoridation of water. *Separation And Purification Technology*, *394*(137585), 137585.
13. Toledano, M., Aguilera, F. S., Osorio, E., Toledano, R., Gutiérrez-Perales, D., Fernández-Romero, E., et al. (2026 July). Effect of parathyroid hormone doped nanoparticles on multiscale modeling and hydroxyapatite formation at the resin-dentin interface. *Dental Materials*, *42*(7), 1182–1197.
14. Fatima, K., Batool, S., Fu, T., & Wu, J. Antibacterial and anti-biofilm properties of hydroxyapatite nanoparticles enhanced by dopamine functionalization. Nano [Internet]. 2026 June 4;(2650135). Available from: http://dx.doi.org/10.1142/s1793292026501353
15. Soto, K., López-Romero, J. M., Díaz, S. M., Mendez, N. E., & Manzano-Ramírez, A. (2025). In Nanophototherapy (Ed.), *Green inorganic metal nanomaterials for combination nanotherapy: synthesis, advantages, and future perspectives* (pp. 501–523). Elsevier.
16. Tharani, M., & Rajeshkumar, S. (2025). Nanotheranostic Mechanism against Infectious Diseases. Sustainable Nanomaterials for Treatment and Diagnosis of Infectious Diseases. ;155–80.
17. Jayakodi, S., Nagarajan, T., & Kirubakaran, D. (2025). Selenium nanoparticles (SeNPs) in cancer therapy: Revolutionizing drug delivery and overcoming treatment challenges. Biomed Mater Devices [Internet]. ; Available from: http://dx.doi.org/10.1007/s44174-025-00586-w
18. Parveen, K., Banse, V., & Ledwani, L. (2016). Green synthesis of nanoparticles: Their advantages and disadvantages. In American Institute of Physics; Available from: http://dx.doi.org/10.1063/1.4945168
19. Green, & Synthesis its Characterization and Antimicrobial Activities of Zinc Oxide Nanoparticles from Silybum marianum Seeds Extract.
20. Tharani, M., Rajeshkumar, S., Al-Ghanim, K. A., Nicoletti, M., Sachivkina, N., & Govindarajan, M. (2023). Terminalia chebula-Assisted Silver Nanoparticles: Biological Potential, Synthesis, Characterization, and Ecotoxicity. Biomedicines [Internet]. ;11(5). Available from: http://dx.doi.org/10.3390/biomedicines11051472
21. Nethi, S. K., Mukherjee, A., & Mukherjee, S. (2026). Biosynthesized gold and silver nanoparticles in cancer theranostics. *Handbook of Nanomaterials and Nanocomposites for Energy and Environmental Applications* (pp. 1–15). Springer Nature Switzerland.

22. Laaradia, M. A., Ettitaou, A., Oubella, K., Laadraoui, J., Gabbas, Z. E., Housseini, A. E. L., et al. (2026 June). Evaluation of anti-inflammatory and analgesic effects of Calendula officinalis extracts in mice. *Uttar Pradesh J Zool*, *8*(11), 48–58.
23. Neelam, A. A., Aliyu, A., Bulle, A. I., Raj, S., & Kumar, M. A brief review exploring the current and traditional therapeutic potential of Calendula officinalis. Int J Drug Deliv Technol [Internet]. 2026 June 8;16(47s). Available from: http://dx.doi.org/10.25258/ijddt.16.47s.110
24. Formulation (2026). and evaluation of a polyherbal nanoparticle-loaded in situ ophthalmic gel containing camellia sinensis and Ocimum sanctum. Iconic Res Eng J [Internet]. ;9(11). Available from: http://dx.doi.org/10.64388/irev9i11-1717609
25. Synergistic antioxidant and antidiabetic activities of Tinospora cordifolia and Azadirachta indica extracts supported by in-silico molecular docking and ADMET evaluation.
26. Shakerimoghaddam, A., Majeed, H. J., Hashim, A. J., Abed, M. J., Jasim, L. S., & Salavati-Niasari, M. (2025). Green synthesis and characterization of NiO/Hydroxyapatite nanocomposites in the presence of peppermint extract and investigation of their antibacterial activities against Pseudomonas aeruginosa and Staphylococcus aureus. *Results in Chemistry*. ;13.
27. Govindan, S. K., Kesavan, L., Selvaraj, R. P., & Karunakaran, G. (2025). *Therapeutic Plant Extract-Mediated Green Synthesis of Hydroxyapatite Nanoparticles for Biomedical Applications. InTherapeutic Plants: Recent Advances in the Use of Herbs as Alternative Medications*. Bentham Science.
28. Lubojański, A., Zakrzewski, W., Samól, K., Bieszczad-Czaja, M., Świtała, M., Wiglusz, R., et al. (2024). Application of nanohydroxyapatite in medicine-A narrative review. *Molecules*, *29*(23), 5628.
29. Nivetha, S., & Sripriya, R. (2026). Green Synthesis of Hydroxyapatite using Chrysopogon zizanioides and Delonix regia for Antibacterial Applications. Mater Circ Econ [Internet]. ;8(1). Available from: http://dx.doi.org/10.1007/s42824-026-00233-9
30. Rekha, M. M., Ojha, V., Mewada, B., Gupta, S., Chinnathambi, A., Alahmadi, T. A. (2024). Green Synthesis of Hydroxyapatite Nanoparticles Using Semecarpus anacardium Linn leaf Extract: Examination of Anticancer Activity and its Apoptosis Induction. J Inorg Organomet Polym Mater [Internet]. ; Available from: http://dx.doi.org/10.1007/s10904-024-03448-y
31. Dragomir, B. R., Robu, A., Bita, A-I., & Sipu, D. (2026). Bioactive hydroxyapatite–collagen composite dressings for wound regeneration: Advances in fabrication, functionalization and antimicrobial strategies. *Appl Sci (Basel)*, *16*(2), 576.
32. Upadhyay, A., Kayal, D., Mandal, S., Tripathi, S., Parmar, A. S., Kumar, K., et al. (2026). Fabrication of 3D-printed adhesive microneedle patch loaded with codoped hydroxyapatite in deep-tissue infective wound healing. *Acs Applied Materials & Interfaces*, *18*(5), 7962–7980.
33. Fadilah, N. I. M., Isa, I. L. M., Zaman, W. S. W. K., Tabata, Y., & Fauzi, M. B. (2022). The effect of nanoparticle-incorporated natural-based biomaterials towards cells on activated pathways: A systematic review. *Polymers (Basel)*, *14*(3), 476.
34. Appasamy, M., Kirubaharan, P., Sulluru, V., Palaniyandi, T., Baskar, G., & Wahab, M. R. (2025). MicroRNA-mediated modulation of signalling pathways in lung cancer: implications for diagnosis

and treatment. *The Journal of Basic and Applied Zoology*, *86*(1), 94.

35. Palanisamy, C. P., Poompradub, S., Sansanaphongpricha, K., Jayaraman, S., Subramani, K., & Sonsudin, F. (2024 Sept). Increased expression levels of PDGF and VEGF magnify the wound healing potential facilitated by biogenic synthesis of silver nanoparticles. Nano-struct Nano-Objects. ;39(101236):101236.
36. Ilango, B., Palaniyandi, T., Baskar, G., Surendran, H., Rab, S. O., & Saeed, M. (2025 Aug). Natarajan Exosomes in cancer: innovative modification strategies for diagnostics and targeted therapy. *Journal of Drug Delivery Science and Technology*, *6*, 107381.
37. Baskar, G., Palaniyandi, T., Al-Mutiry, M., Alshammari, N., & Saeed, M. (2025 Oct). Biocatalytic Green Synthesis of Iron Oxide Nanoparticles Using Red Seaweed Portieria hornemannii for Biomedical Applications. *Biocatalysis and Agricultural Biotechnology*, *24*, 103831.
38. Zhou, Z., Cao, R., Shi, L., & Jin, W. (2026). Mechanisms underlying the role of TNF-α and IL-1β preconditioned exosomes derived from human umbilical cord mesenchymal stem cells in wound healing. *Frontiers In Immunology*, *17*(1713004), 1713004.
39. Rembe, J-D., Garabet, W., Augustin, M., Dissemond, J., Ibing, W., Schelzig, H., et al. (2025). Immunomarker profiling in human chronic wound swabs reveals IL-1 beta/IL-1RA and CXCL8/CXCL10 ratios as potential biomarkers for wound healing, infection status and regenerative stage. *J Transl Med*, *23*(1), 407.

# Figures

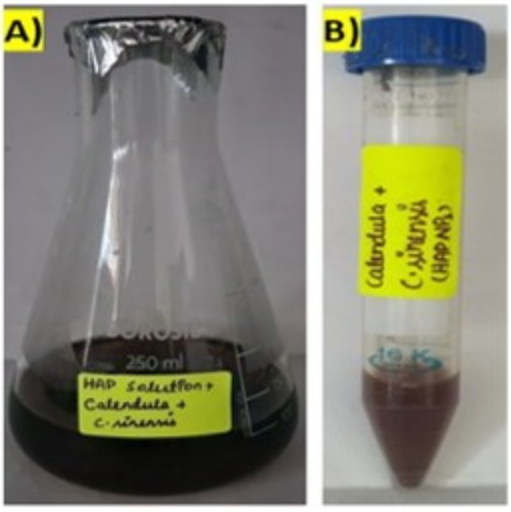



**Figure 1**

**Green synthesis of Calendula and *Camellia sinensis*-mediated hydroxyapatite nanoparticles (HAp NPs). A) Formation of HAp nanoparticles indicated by visible colour change B) HapNPs pellet**

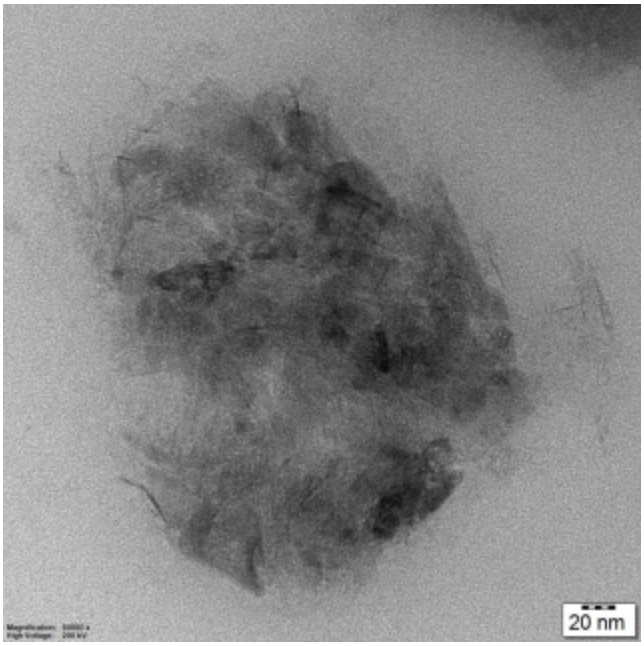



**Figure 2**

**Transmission electron microscopic image of synthesized hydroxyapatite nanoparticles**

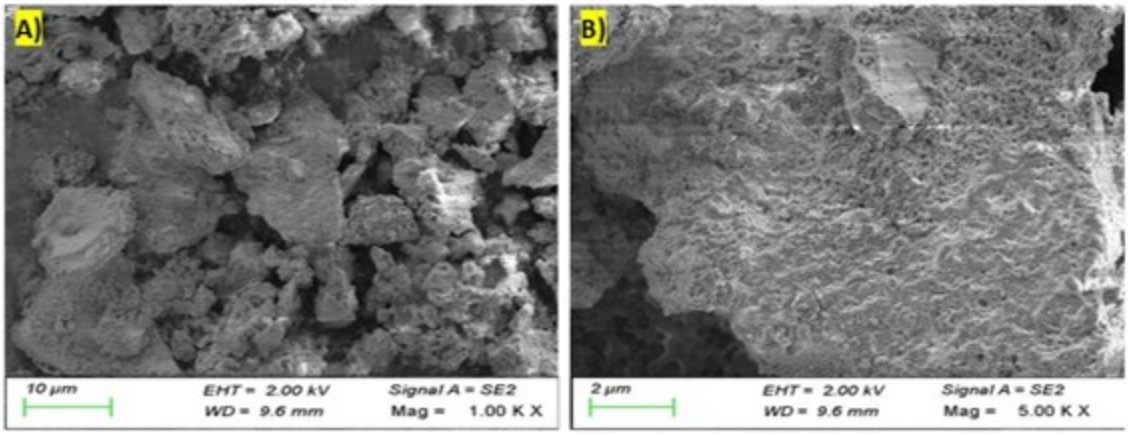



**Figure 3**

**SEM micrographs of synthesized hydroxyapatite nanoparticles (A) Low-magnification image at 10 µm (B) Higher-magnification image at 2 µm**

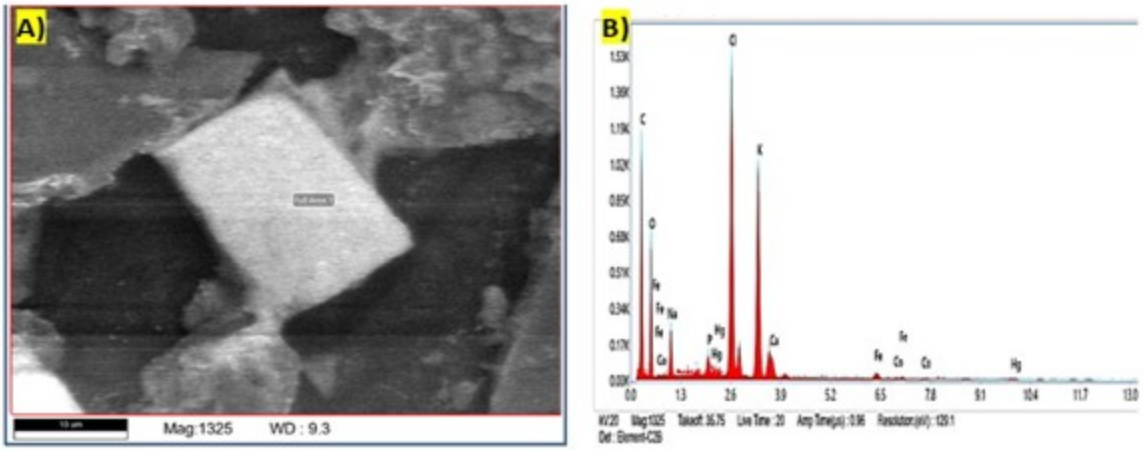



**Figure 4**

**SEM–EDX analysis of synthesized hydroxyapatite nanoparticles. (A) SEM image (B) EDX spectrum**

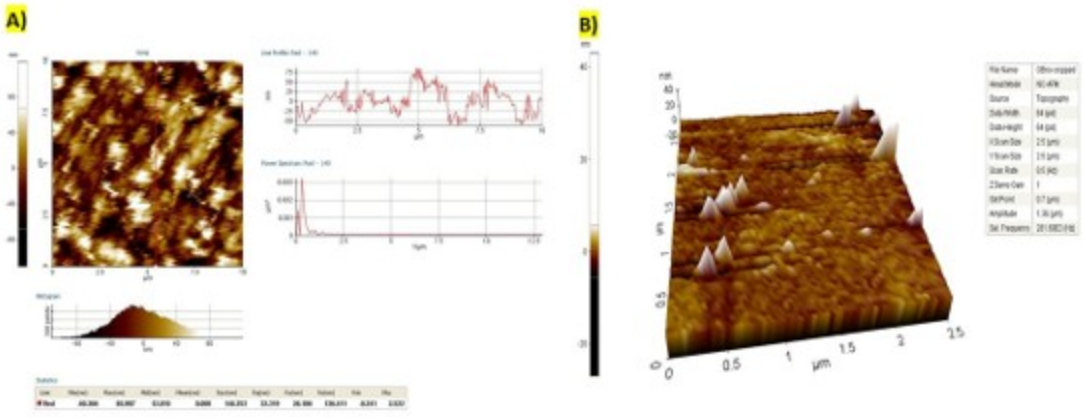



**Figure 5**

AFM analysis of synthesized hydroxyapatite nanoparticles. (A) Two-dimensional AFM image showing rough, granular, irregular morphology and distribution of height and roughness. (B) Three-dimensional AFM image showing rough surface structure with peaks and valleys indicating heterogeneous surface arrangement of nanoparticles.

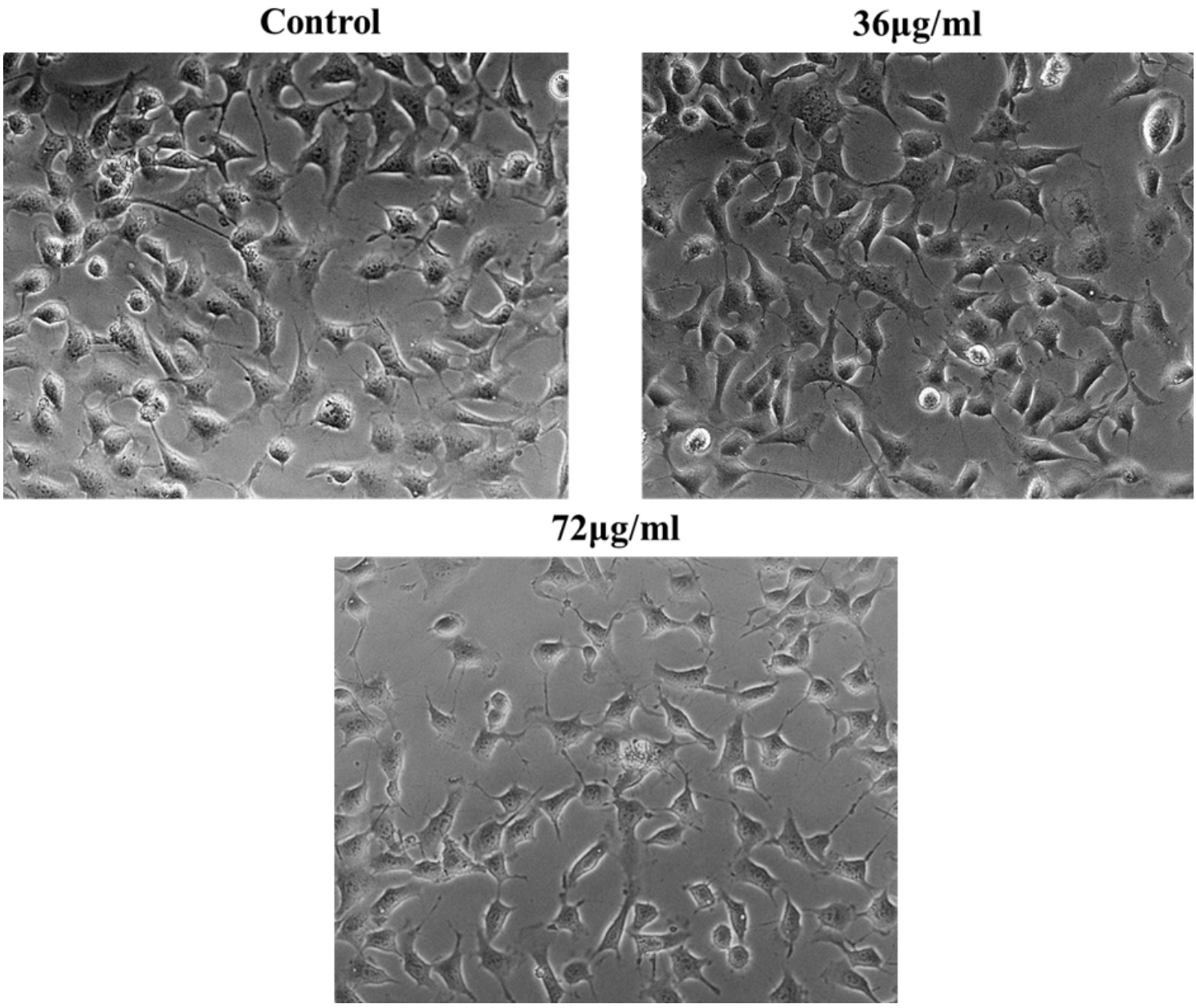



**Figure 6**

**Biocompatibility assessment of hydroxyapatite nanoparticles using cell morphology analysis. (A) Untreated control cells (B) Cells treated with hydroxyapatite nanoparticles at 36 µg/mL (C) Cells treated with hydroxyapatite nanoparticles at 72 µg/mL.**

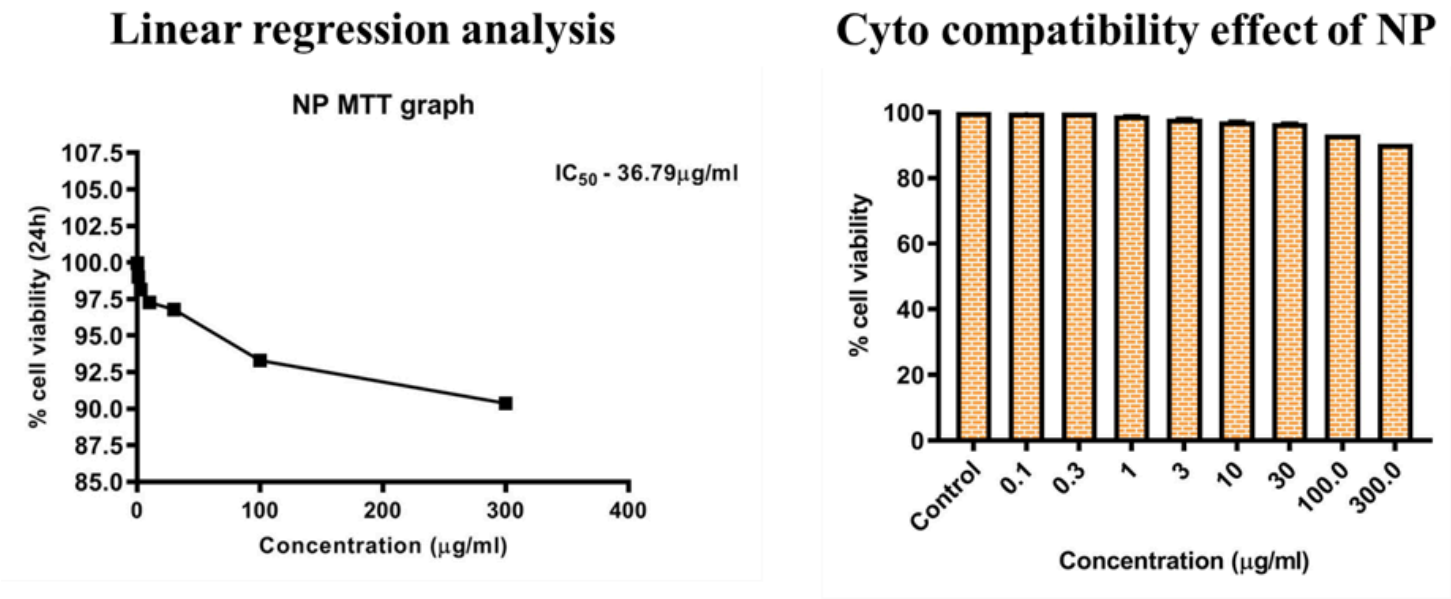



Figure 7

**Cytocompatibility analysis of hydroxyapatite nanoparticles by MTT assay. (A) Linear regression analysis (B) Percentage cell viability of cells treated with different concentrations of hydroxyapatite nanoparticles**

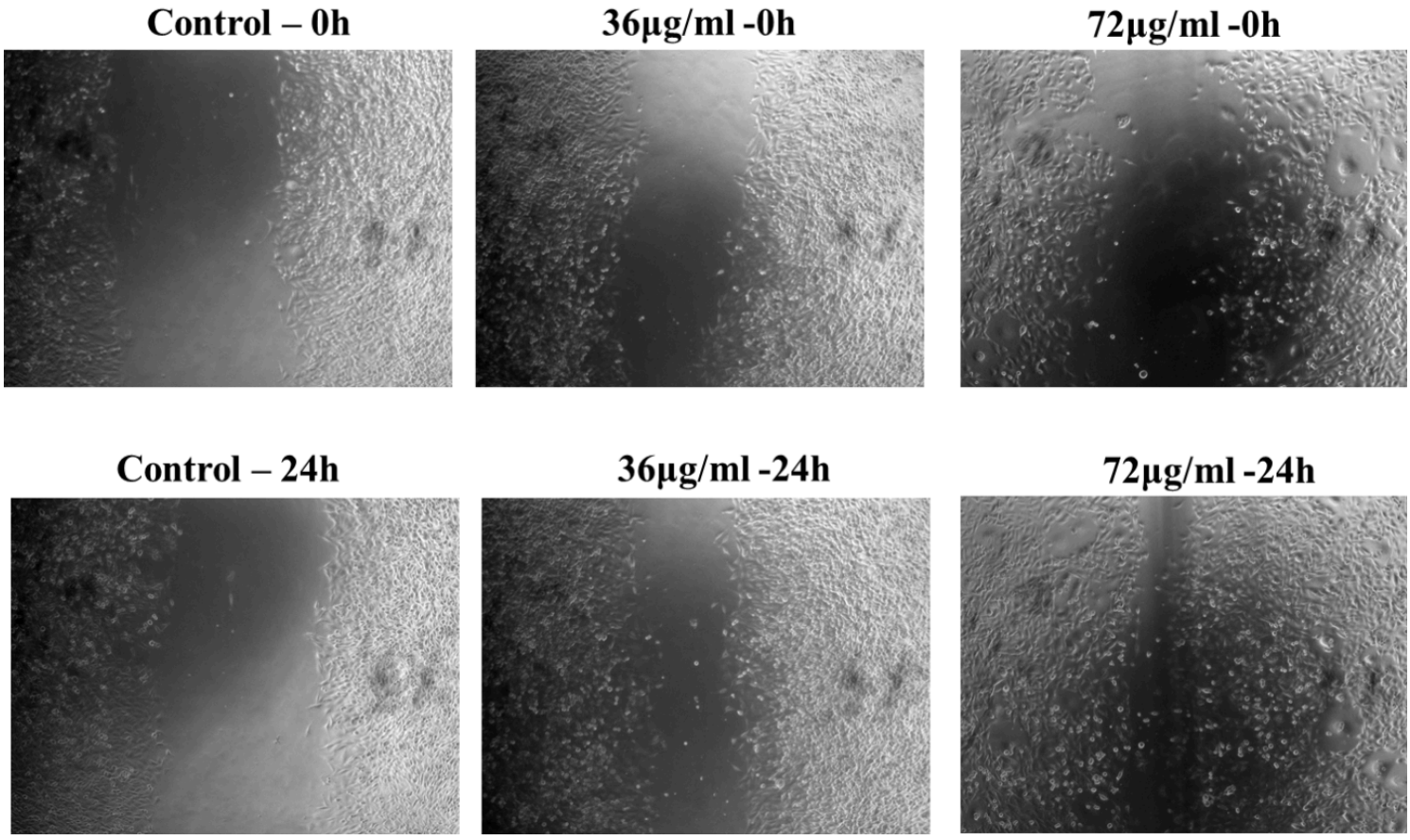



Figure 8

**Morphometric analysis of in vitro scratch wound healing assay of hydroxyapatite nanoparticles in a cell line model. (A) Control, initial gap at 0 hour. (B) 0 hour, cells exposed to hydroxyapatite nanoparticles 36 µg/mL. (C) 0 hour, cells exposed to hydroxyapatite nanoparticles 72 µg/mL. (D) Control, 24 hour, partial closure. (E) 24 hour, cells exposed to hydroxyapatite nanoparticles 36 µg/mL, enhanced cell migration, reduced gap. (F) 24 hour, cells exposed to hydroxyapatite nanoparticles 72 µg/mL, significant closure compared to control.**

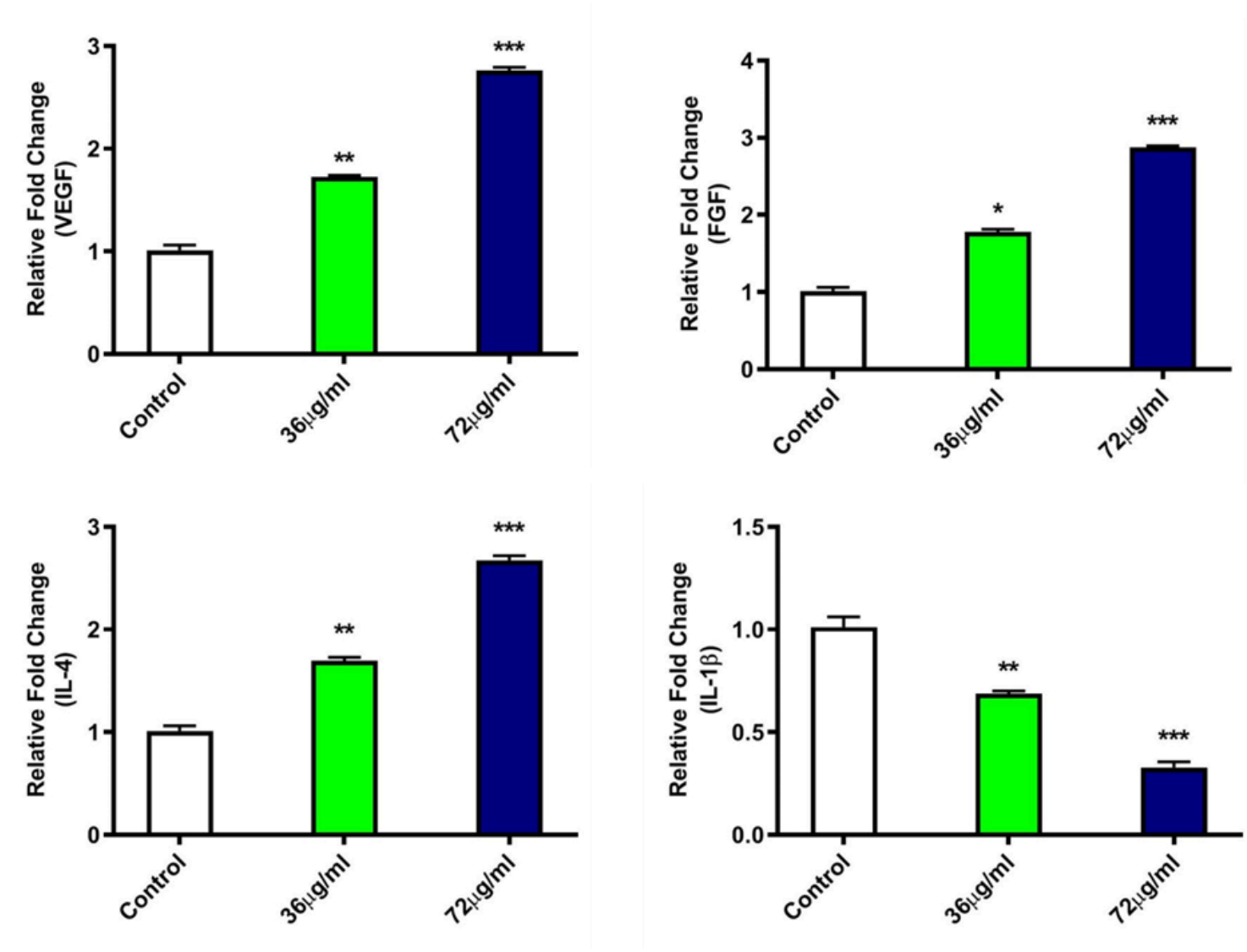



Figure 9

**Gene expression of wound healing and inflammatory markers in hydroxyapatite nanoparticle-treated cells. (A) Upregulation of vascular endothelial growth factor (VEGF) in a dose-dependent manner is shown as relative fold change. (B) Expression of fibroblast growth factor (FGF) is shown as relative fold change in a treated group. (C) Relative fold change of interleukin 4 (IL-4) is shown as an increase of an anti-inflammatory marker. (D) Relative fold change of interleukin 1 beta (IL-1β) is dose-dependently reduced after treatment. Data are expressed as mean ± SD. Statistically significant changes are indicated as *p < 0.05, **p < 0.01, and ***p < 0.001 compared to control.**